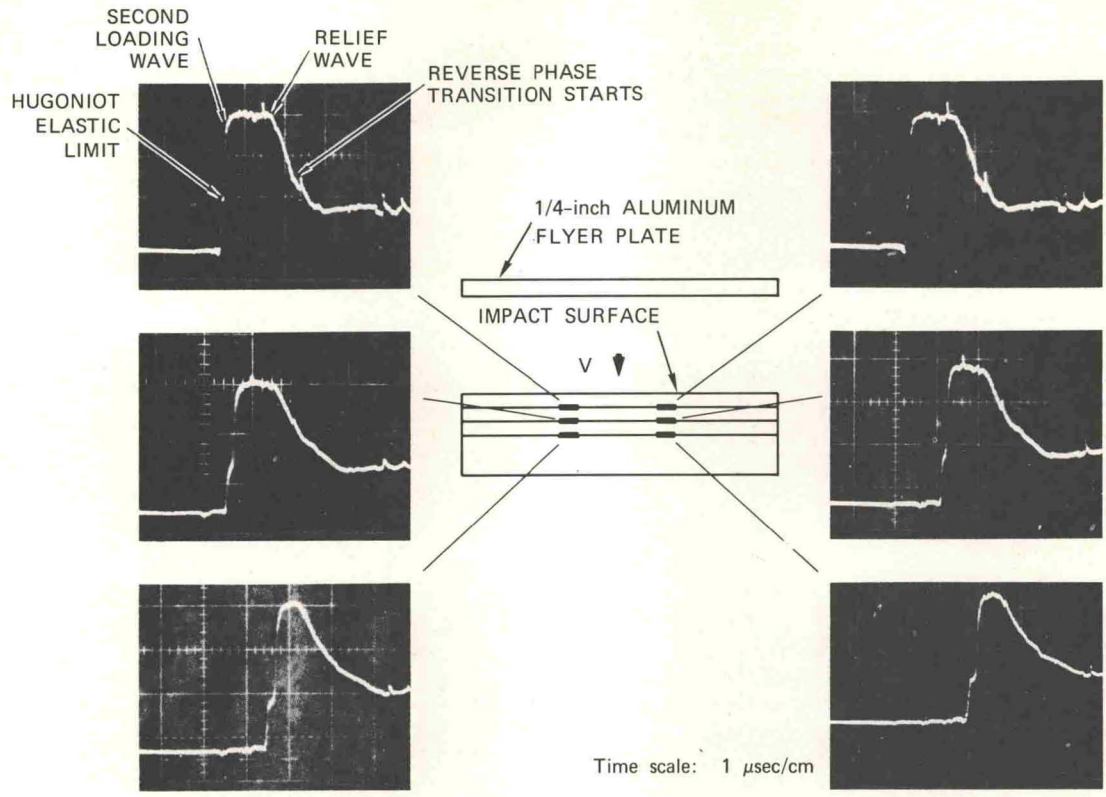

Fig. 2. Manganin stress gage profiles in Arkansas novaculite. Peak stress of 252 kbar.

is into a region of constant state (simple wave) $C_\sigma = C_u = C$ and the stress volume history reduces to a single integral [*Cowperthwaite and Williams*, 1971],

$$V = V_H - \int_{\sigma_H}^{\sigma} \frac{d\sigma}{\rho_0^2 C^2} \tag{3}$$

Time correlation between experimental records was a weak point in the present work and the primary source of scatter in the Hugoniot data points shown in Figure 3. Before (3) was used to determine unloading behavior of the material, the present Hugoniot data with those of *Ahrens and Rosenberg* [1968] and *Wackerle* [1962] in the mixed phase region were fit to an analytic function. The fitted Hugoniot is shown in Figure 3 as a solid line. This Hugoniot was used to provide better time correlation between experimental profiles. This procedure is reasonable. Values for the shock velocity in this stress region are not in question. It is the relief velocities as a function of stress that determine the unloading path.

TABLE 1. Arkansas Novaculite: Shock Wave Data

	Elastic				Plastic			
Shot	C_e, mm/μs	σ_e,* kbar	U_e, mm/μs	V_{hel}, cm³/g	U_s, mm/μs	σ_H, kbar	U_H, mm/μs	V_H, cm³/g
8909-1†	...	...	...	...	6.3	444	2.60	0.218
1883-4	6.20	90	0.552	0.346	5.40	252	1.94	0.268
1883-16	6.05	95	0.597	0.343	5.45	352	2.39	0.218
1883-17	6.24	85	0.52	0.348	5.70	222	1.43	0.287
1883-6	6.20	70	0.425	0.135	5.60	241	1.63	0.272
1883-7	6.00	98	0.62	0.341	5.50	252	1.68	0.268
8909-2	6.03	79	0.50	0.349	5.45	301	2.10	0.234

*Average of six gages (trend of decay with distance ~4-5 kbar over 6 mm).
†Elastic wave was overdriven.

The complete stress-volume paths are shown in Figure 4. The Hugoniot jump conditions were used to determine the loading paths, and (3) was used to determine the relief path.

It was assumed that the quartz relieved to zero stress after shock reflection from the aluminum flyer free surface. The assumption is reasonable, since the quartz relief adiabats determined from this work are steeper than similar adiabats for aluminum. No experiments were performed to justify this assumption. If the manganin gage level after relief corresponded to some residual stress, the effect on the predicted relief path would be small at the top of the relief and would become progressively more pronounced at lower stresses. The overall effect would be to shift the unloading paths slightly to the right in Figure 4. Also, the predicted level at which the reverse phase change is expected to proceed would be higher (~120 kbar). The best indication that a stress level close to zero was obtained upon first relief comes from the gage records. A number of gages survived a sufficient length of time to have shown a second reverberation relief from the flyer free surface; no clear indication of a second relief wave was observed.

The steep relief behavior in quartz has been observed in earlier work by *Ahrens and Rosenberg* [1968], where optical methods and shock reflection techniques provided estimates of the relief behavior. *Butkovich* [1971] found that prediction of peak stress attenuation with range in the Benham event required large hysteresis in the constitutive model of the quartz rock. The present work provides independent corroboration of this previous work.

In Figure 4, principal isentropes (hydrostatic) for α quartz and stishovite are shown. The isentrope shown for

α quartz is a Murnaghan equation fit to acoustic data [*Anderson*, 1966] and is consistent with static data of *McWhan* [1967]. The α quartz isentrope has been extrapolated beyond the pressure at which α quartz is expected to undergo polymorphic phase transformation to stishovite. The stishovite isentrope shown is also a Murnaghan equation fit. The parameters were determined by *Ahrens et al.* [1970] from shock wave and thermodynamic data. These isentropes determine the region of mixed phase in the pressure-volume plane.

To understand the unloading behavior in the mixed phase region, three curves of frozen concentration corresponding to 25, 50, and 75% stishovite are shown. The curves were obtained by constant specific volume ratios between the principal isentropes of α quartz and stishovite. Thermodynamically, pressure, temperature, and particle velocity equilibriums are assumed between phases, and surface energies are ignored. Although the lever rule is strictly valid only for isotherms, differences between α quartz and stishovite isotherms and isentropes are negligible up to pressures better than 300 or 400 kbar. Finally, the principal isentrope for stishovite shown in Figure 4 and that reached under shock compression from the α quartz initial specific volume differ slightly. Despite the number of assumptions required the curves obtained are reasonably close to paths of frozen concentration and provide a reference frame for examining the experimental unloading behavior. Our conclusion is that after partial or complete transformation to the high-density phase, material unloading occurs along, or close to, paths of frozen concentration down to about 80 kbar.

Particle velocity gage experiments. The previous experiments using flyer plate impact do not indicate a continuing quartz to stishovite phase transformation after the initial shock has placed the material in the mixed quartz-stishovite metastable region. The in-contact explosive experiments provided an unloading rate, after shock loading, substantially less than that obtained in the flyer plate experiments. We attempted to observe a continuing phase transformation rate within this longer experimental time scale.

The Taylor wave produces a decaying triangular particle velocity profile in the material, as the profiles obtained from one of two similar experiments shown in Figure 5 indicate. The initial unloading rate observed was about 10 kbar/μs, or better than 2 orders of magnitude lower than unloading rates in the flyer plate experiments. The sudden acceleration observed in Figure 5 occurs when the relief wave from the target free surface reaches the gage planes.

In Figure 6, three particle velocity profiles are shown that idealize the experimental data during initial unloading. The particle velocity field is determined by the shock velocity U, the slope of individual profiles a, and the slope of the decaying shock front b. The following analysis determines the initial unloading stress-volume path in the mixed phase region in terms of these parameters. Comparison with paths of frozen quartz-stishovite phase concentration determines whether the α quartz to stishovite transformation is continuing behind the shock front in the time span of the Taylor relief wave.

The particle velocity field behind the shock can be written

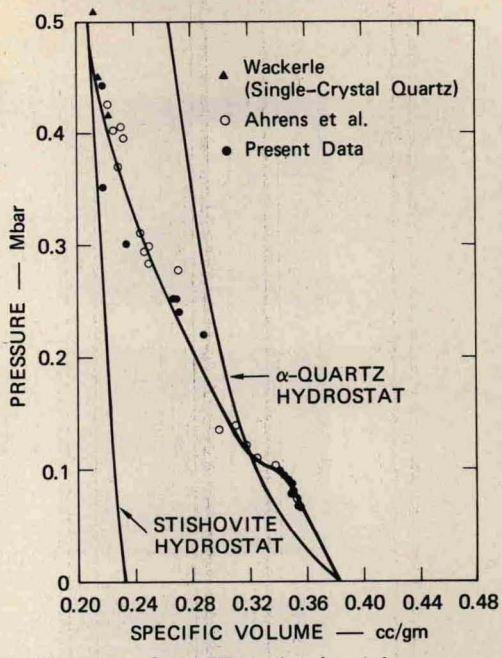

Fig. 3. Pressure-volume Hugoniot for Arkansas novaculite.

$$u(h, t) = u_0 + at + \frac{b - a}{U} h \tag{4}$$

where u_0 is the initial particle velocity magnitude of the first profile at zero time (arrival of the shock wave at the first gage) and h is the Lagrangian coordinate. The initial stress-volume path can be determined by obtaining the velocities of constant stress and particle velocity levels C_σ and C_u and using the relation [*Fowles and Williams*, 1970]

$$d\sigma/dV = -\rho_0^2 C_u C_\sigma \tag{5}$$

Equation 6 is obtained by using (4) and $C_u = (\partial h/\partial t)_u$:

$$C_u = \frac{a}{a - b} U \tag{6}$$

Equation 7 is obtained from (4) by using $C_\sigma = (\partial h/\partial t)_\sigma$ and the Hugoniot jump condition:

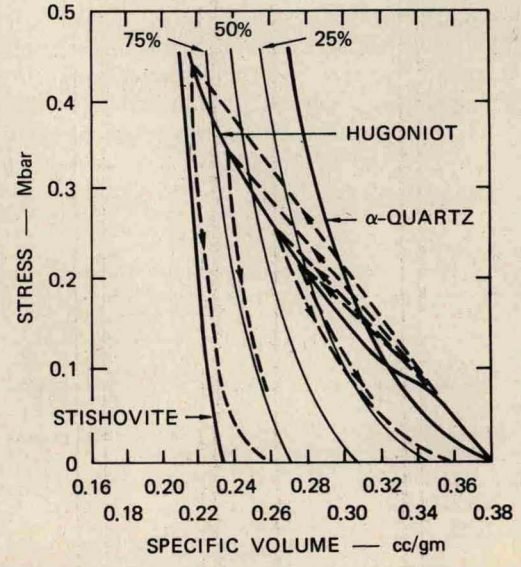

Fig. 4. Stress-volume relief paths in Arkansas novaculite. Loading and relief paths are indicated by the dashed lines.